GENOMICS 27, 389–398 (1995)

cDNA Cloning, Tissue Distribution, and Chromosomal Localization of *Ocp2*, a Gene Encoding a Putative Transcription-Associated Factor Predominantly Expressed in the Auditory Organs

HONG CHEN, ISOLDE THALMANN,* JOE C. ADAMS,† KAREN B. AVRAHAM,‡ NEAL G. COPELAND,‡ NANCY A. JENKINS,‡ DAVID R. BEIER,§ DAVID P. COREY,¶ RUDI THALMANN,* AND GEOFFREY M. DUYK[1]

*Howard Hughes Medical Institute and Department of Genetics, and §Genetics Division, Brigham Women's Hospital, Harvard Medical School, Boston, Massachusetts 02115; †Department of Otolaryngology, Massachusetts Eye and Ear Infirmary, and ¶Howard Hughes Medical Institute and Department of Neurology, Massachusetts General Hospital, Boston, Massachusetts 02114; *Department of Otolaryngology, Washington University, St. Louis, Missouri 63110; and ‡Mammalian Genetics Laboratory, ABL-Basic Research Program, NCI-Frederick Cancer Research and Development Center, Frederick, Maryland 21702*

Received January 5, 1995; accepted March 27, 1995

We report the cloning of the *Ocp2* gene encoding OCP-II from a guinea pig organ-of-Corti cDNA library. The predicted open reading frame encodes a protein of 163 amino acids with an estimated molecular mass of 18.6 kDa. A homology search revealed that *Ocp2* shares significant sequence similarity with p15, a subunit of transcription factor SIII that regulates the activity of the RNA polymerase II elongation complex. The *Ocp2* messenger RNA is expressed abundantly in the cochlea while not significantly in any other tissues examined, including brain, eye, heart, intestine, kidney, liver, lung, thigh muscle, and testis, demonstrating that the expression of this gene may be restricted to auditory organs. A polyclonal antiserum was raised against the N-terminal region of OCP-II. Immunohistochemical staining of paraffin-embedded sections of the cochlea showed that OCP-II is localized abundantly in nonsensory cells in the organ of Corti; in addition, it was also detected, at a lower concentration, in vestibular sensory organs, as well as auditory and vestibular brain stem nuclei. The *Ocp2* gene was mapped to mouse chromosome 4 as well as 11. Our results suggest that OCP-II may be involved in transcription regulation for the development or maintenance of specialized functions of the inner ear.

INTRODUCTION

The auditory organ of mammals, the cochlea, is a snail-shaped organ enclosed by the temporal bone. Within the cochlea sound stimulation produces motion of the basilar membrane, upon which rest sensory hair cells and associated cells that comprise the organ of Corti, the auditory sensory transduction apparatus. The extraordinary sensitivity of the organ of Corti is made possible by a unique ionic and electrochemical environment, wherein the apical surfaces of the hair cells are bathed in endolymph, an extracellular fluid characterized by ion contents very similar to those of intracellular fluids. The receptor potentials of hair cells are carried by potassium ions (Corey and Hudspeth, 1979), which flow from the endolymphatic space through the hair cells in response to vibrations of the basilar membrane. A feature of the vertebrate cochlea not found in other hair cell organs is the presence of a positive resting potential of 80–100 mV, the endolymphatic potential, between the endolymphatic space and the surrounding tissue. The endolymphatic potential is crucial for the sensitivity shown by the organ of Corti, and it presents special problems for the maintenance of physiological pH and for recycling potassium ions back into the endolymph up the electrochemical gradient (see reviews by Sterkers, 1985; Marcus, 1986; Salt and Konishi, 1986).

In view of the highly specialized nature of hair cell organs and of the peculiar electrochemical environment within the cochlea, one might expect specific molecular mechanisms to be involved in the functions of this environment. Using two-dimensional gel electrophoresis with materials from microdissected guinea pig organ of Corti, two low-molecular-weight proteins were found in extremely high concentrations in the organ of Corti. These two proteins, named OCP-I and OCP-II, have molecular masses of 37 and 22.5 kDa, respectively (Thalmann *et al.*, 1980). The two proteins are also present, at much lower levels, in the vestibular organs and

Sequence data from this article have been deposited with the EMBL/GenBank Data Libraries under Accession No. Z35481. *Ocp2-rs1*, MGD-CREX-223. *Ocp2-rs2*, MGD-CREX-224.

[1] To whom correspondence should be addressed at Millennium Pharmaceuticals Inc., 640 Memorial Drive, Cambridge, MA 02139. Telephone: (617) 374-9480. Fax: (617) 374-9379.

0888-7543/95 $6.00

a variety of other inner ear tissues, but were not observed in any other tissues examined by 2-D gel electrophoresis (Thalmann *et al.*, 1990). The partial amino acid sequence of OCP-II was obtained by peptide sequencing (Thalmann *et al.*, 1993). The highly abundant and apparently localized expression pattern of these two proteins implies that they may play important roles in the function of the organ of Corti.

One difficulty in studying the organ of Corti is the extremely limited amount of material available from each organ. Isolation of genes specifically expressed in the organ of Corti is an important step to the full understanding of their biological function in the organ of Corti. Here we report the cloning and sequence analysis of the *Ocp2* gene encoding OCP-II, studies of the expression of *Ocp2* in various tissues, the cellular localization of OCP-II in the inner ear, and the mouse chromosome location of *Ocp2*. The possible function of OCP-II, based on these studies, will be discussed.

MATERIALS AND METHODS

Primers for degenerate RT-PCR and sequencing. The set of degenerate primers was designed according to the published partial amino acid sequence of OCP-II (Thalmann *et al.*, 1993). All oligos were synthesized at the Biopolymer Facility in Harvard Medical School (Boston, MA). Oligos are shown from 5′ to 3′ using nucleotide numbers as assigned in Fig. 1. OCPIIA, GA(CT) GGN GA(AG) AT(ACT) TT(CT) GA(AG) GTN GA (nucleotides 132–154); OCPIIB, GT NCC (TC)TG (AG)TC NAC (TC)TT (nucleotides 400–384). Primers used in library screening and sequencing of *Ocp2:* OCPIIAF, GAC CAT GTT GGA AGA TTT GGG (nucleotides 188–198); OCPIIAB, TGG TAG AGG AAC TGG GTC ATC (nucleotides 248–228); OCPII9F, CTC CTG AGG AGA TTC GCA AGA C (nucleotides 496–517); OCPII10, CAG GAA TTC TTG GTC CC (nucleotides 383–367); OCPII20F, GGC TAC TTG AAG TAA CTA TTC C (nucleotides 928–949); OCPII20B, CTT GGA ATA GTT ACT TCA AGT AG (nucleotides 952–930); OCPII30F, TGA ACT GTG GGT TCT GTG TAG (nucleotides 747–767); OCPIIML2, TAG AAG GGT TGT TCC AAA TGC; and OCPIIMR1, TGC CAC TTT CCG CAG AGA AC. A pair of primers against the guinea pig cytochrome P450 reductase cDNA (Accession No. D10498) were used as positive control for the RT-PCR: 450RL, CTC CCA CGT GGA CAC CGG TG (nucleotides 28–47); and 450RR, ACT TGA CAC CAG AGA GGT CC (nucleotides 521–502).

PCR conditions. The 25-μl PCR reaction contained 2 m*M* $MgCl_2$, 1 μ*M* each primer, 250 μ*M* each dATP, dTTP, dCTP, and dGTP, and 0.5 units of *Taq* polymerase in 1× Mg-free *Taq* polymerase buffer (Promega Corp., Madison, WI). All PCR reactions were performed in the GeneAmp PCR System 9600 from Perkin–Elmer Corp. (Norwalk, CT). Unless otherwise described, the general PCR profile was 94°C, 3 min, 94°C, 15 s, 57°C, 15 s, 72°C, 60 s for 35 cycles and 72°C, 5 min for 1 cycle. The degenerate PCR profile was 94°C, 3 min, 94°C, 30 s, 42°C, 30 s, 72°C, 60 s for 35 cycles and 72°C, 5 min for 1 cycle as previously described (Compton, 1990).

cDNA synthesis. Small-scale total RNA was prepared from up to 100 mg of guinea pig brain, eye, heart, intestine, kidney, liver, lung, thigh muscle, and testis by the method of Chomczynski and Sacchi (1993). Six cochleae were used for RNA preparation. One microgram of total RNA from each tissue and all RNA prepared from the 6 cochleae (<1 μg) were reverse-transcribed into cDNA using 40 ng random $pd(N)_6$ (Boehringer Mannheim, Indianapolis, IN) with the Superscript reverse-transcriptase from GIBCO BRL (Gaithersburg, MD) following the manufacturer's manual. After precipitation with ethanol, cDNA was dissolved into 200 μl dH_2O. For RT-PCR, an equal amount of cDNA from each sample was used as template in a 25-μl PCR reaction under the conditions described above. Primers OCPIIAF and OCPII10 were used for the amplification.

cDNA library screening. The organ of Corti cDNA library from guinea pig was kindly provided by Drs. Wilcox and Fex (NIH). It was constructed with the pSport1 vector (Wilcox and Fex, 1992). The library (5×10^6 colonies) was plate-amplified and saved into 96 pools in 15% glycerol at −70°C. Plasmid DNA was prepared from each pool. The DNA pools were first screened with a set of *Ocp2* primers OCPIIAF and OCPII10 from the cloned region that gave a 196-bp fragment. Two pools with the strongest positive signals were then plated on two LB plates (200,000 colonies/plate) containing ampicillin (100 μg/ml) and incubated overnight at 37°C. Two nylon membranes (Micron Separations, Westboro, MA) were subsequently overlaid on each plate and transferred onto new LB plates. Both the original plates and the plates with the membranes were incubated at 37°C for 5 h. Membranes were then placed on top of Whatman3 soaked with 5% SDS/2× SSC for 2 min, microwaved for 2.5 min, and soaked in 5× SSC to wipe away the colonies. They were prehybridized in 100 ml prehybridization solution (6× SSC, 5× Denhardt's, 0.05% Na pyrophosphate, 0.5% SDS, and 100 mg/ml boiled salmon sperm DNA) at 37°C for 3 h and hybridized in 20 ml hybridization solution (6× SSC, 1× Denhardt's, 0.05% Na pyrophosphate, and 100 mg/ml boiled salmon sperm DNA) at 48°C overnight. The probe was 30 ng of the subcloned *Ocp2* fragment radiolabeled using the oligolabeling kit from Pharmacia LKB (Uppsala, Sweden). Filters were washed subsequently twice in 2× SSC/0.5% SDS for 5 min at room temperature, once in 2× SSC/0.1% SDS for 20 min at room temperature, and twice in 0.1× SSC/0.5% SDS for 20 min at 55 and 65°C, respectively. The filters were exposed to X-ray film (Eastman Kodak Company, Rochester, NY) at −70°C overnight.

Sequence analysis. DNA sequencing was performed on automatic ABI 373A DNA sequencer by using the *Taq* cycle sequencing kit (Applied Biosystems, Foster City, CA). T3, T7, Sp6, and M13 reverse primers, as well as custom made primers, were used with purified plasmids. Sequence analysis was performed using the GCG Sequence Analysis Software Package (Genetics Computer Group, Madison, WI).

In vitro transcription, translation, and immunoprecipitation. The cloned *Ocp2* plasmid pSpoocp2A (~1.4 kb) was analyzed by *in vitro* transcription and translation. Two micrograms of purified plasmid was transcribed into RNA with T7 RNA polymerase (total volume of 20 μl) using the MEGAscript kit from Ambion (Austin, TX). Two microliters of the 1:10 diluted RNA was then used in the NEN reticulocyte lysate, L-[^{35}S]methionine translation system (DuPont NEN). Immunoprecipitation was performed essentially as described by Jiang *et al.* (1994) with slight modifications: 2 μl of the above 25-μl *in vitro* translation product was mixed with 98 μl protein lysis buffer (5 m*M* Tris, 1 m*M* EDTA, 10% SDS, pH 7.5) and boiled for 3 min. The lysate was immunoprecipitated at 4°C for 1 h with 10 μl rabbit anti-OCP-II polyclonal antibody in 400 μl immunoprecipitation buffer (0.1 *M* NaCl, 0.02 *M* Na borate, 15 m*M* EDTA, pH 8.5, 0.02% Na azide) plus 0.5% Triton X-100 and 0.5% BSA. An antibody against the OCP-II protein was derived from a synthetic tetradecapeptide corresponding to residues 3–16 of the amino acid sequence of OCP-II coupled to keyhole limpet hemocyanin (BAbCO, Richmond, CA). The preimmune serum from the same rabbit served as negative control. Immunoprecipitates were then incubated with 30 μl 1:1 slurry of protein-A beads for 1 h at 4°C. Immunoprecipitates were washed 4 times with immunoprecipitation buffer plus 0.5% Triton, 0.5 *M* sucrose, 0.1% SDS, and 0.5% BSA and once with the above buffer minus BSA. After denaturation in 20 μl of 2× SDS sample buffer (2% SDS, 100 m*M* dithiothoreitol, 60 m*M* Tris, pH 6.8, 0.01% bromophenol blue) by boiling for 5 min, immunoprecipitates were analyzed by 15% SDS–polyacrylamide gel electrophoresis and fluorography.

Immunoblot. Freeze-dried samples of guinea pig organ of Corti were obtained as described in detail previously (Thalmann, 1976). Each sample (10 μg) was solubilized in 20 μl of 1× sample buffer. After boiling for 5 min, proteins were separated by 15% SDS–polyacrylamide gel electrophoresis and electrophoretically transferred (Towbin *et al.*, 1979) onto NitroBind membranes (Micron Separa-

tions) using protein blotting cells from Bio-Rad Laboratories (Life Science Group, Melville, NY) following the manufacturer's manual. Membranes were incubated in 5% blocking agent (5% Carnation nonfat dry milk, 0.1% Tween in PBS) at room temperature for 1 h, rinsed three times for 5 min in PBS-T (PBS plus 0.1% Tween), incubated in 1:500 diluted preimmune serum, as control, and primary antibody solution, respectively, for 1 h, rinsed three times for 5 min in PBS-T and in 1:5000 diluted secondary antibody anti-rabbit IgG linked alkaline phosphatase (AP) (Pharmacia LKB) for 1 h, rinsed three times with PBS-T and finally in reaction AP buffer (0.165 mg/ml BCIP and 0.33 mg/ml NBT) for 10 min. Membranes were then rinsed with H_2O to stop the reaction and air-dried.

Immunohistochemistry. Guinea pigs were deeply anesthetized and perfused intracardially with body-temperature phosphate-buffered saline (PBS), followed by 10% formalin in PBS. The cochleae were exposed, the staples were removed, the round window was perforated, and fixative was gently perfused through the scalae. An hour later the temporal bones were placed in 120 m*M* EDTA (pH 7.0) and gently agitated until they were decalcified. They were dehydrated in ethanol, embedded in paraffin, cut at 6 μm, and mounted on gelatin subbed slides. Selected sections were dewaxed in xylene, hydrated, and treated with 5% normal horse serum (NHS) for 1 h. Visualization of the antigenic sites was performed using a biotin amplification technique (Adams, 1992), as follows. Sections were incubated in primary antiserum overnight at room temperature. Dilutions of the primary antiserum (in 1% NHS in PBS) ranged from 1:10,000 to 1:2,000,000. After the primary antibody, sections were incubated in biotinylated donkey anti-rabbit antibody for 1 h (1:400, Jackson Immuno Research, West Grove, PA), avidin–biotin–horseradish peroxidase conjugate (Standard ABC kit, Vector, Burlingame, CA) for 1 h, biotinylated tyramine (1:100)–H_2O_2 (0.01%) for 10 min, ABC for 30 min, diaminobenzidine–H_2O_2 (0.01%) for 2–10 min. Copious washing in PBS was performed between each step. Following the colorization reaction sections were dehydrated, cleared in xylene, and coverslipped in Permount. Controls included substituting preimmune serum for the anti-OCP-II or preabsorbing the primary antibody with a OCP-II-GST fusion protein. For the latter 2 m*M* fusion protein was added to the primary antibody, and the mixture was gently agitated overnight. This preabsorbed solution and a nonpreabsorbed antibody at the same dilution were processed in tandem on adjacent sections using samples from common volumes of all other reagents to perform the immunoreaction. Results with the biotin-amplified technique were verified using the more common technique employing a biotinylated secondary antibody, followed by biotin–avidin–peroxidase and then the coloration. The biotin-amplified technique was usually used because it offers several orders of magnitude more sensitivity over which to test for staining of sites with less immunoreactivity.

Mapping of Ocp2. Interspecific backcross progeny were generated by mating (C57BL/6J × *Mus spretus*)F_1 females and C57BL/6J males as described (Copeland and Jenkins, 1991). A total of 205 N_2 mice were used to map *Ocp2*. DNA isolation, restriction enzyme digestion, agarose gel electrophoresis, Southern blot transfer, and hybridization were performed as described (Jenkins *et al.*, 1982). All blots were prepared with Hybond-N^+ membrane (Amersham Life Sciences, Arlington Heights, IL). The probe, a 270-bp mouse genomic clone, was labeled with [α^{32}P]dCTP using random priming (Amersham). Fragments of 8.8, 7.4, and 3.5 kb were detected in *Pvu*II-digested C57BL/6J DNA and fragments of 8.8, 4.0, and 2.2 kb in *Pvu*II-digested *M. spretus* DNA. The presence or absence of the 4.0- and 2.2-kb *M. spretus*-specific *Pvu*II fragments, which segregated independently, was followed in the backcross mice. In addition, fragments of 12.0, 5.5, and 4.0 kb were detected in *Pst*I-digested C57BL/6J DNA and fragments of 15.0, 5.5, and 4.6 kb in *Pst*I-digested *M. spretus* DNA. The presence or absence of the 15.0- and 4.6-kb *M. spretus*-specific *Pst*I fragments, which segregated independently, was followed in the backcross mice. The *Pvu*II and *Pst*I RFLP data were combined. The 4.0-kb *M. spretus Pvu*II RFLP and the 4.6-kb *M. spretus Pst*I RFLP were used to follow the segregation of the *Ocp2-rs1* locus in backcross mice. The 2.2-kb *M. spretus Pvu*II RFLP and the 15.0-kb *M. spretus Pst*I RFLP were used to follow the segregation of the *Ocp2-rs2* locus.

A description of the probes and RFLPs for the loci linked to *Ocp2-rs1* and *Ocp2-rs2* has been reported previously, including Gardner–Rasheed feline sarcoma viral oncogene homolog (*Fgr*), leukemia-associated phosphoprotein (*Lag*), natriuretic peptide precursor type A (*Nppa*), adrenergic receptor α_1 (*Adra1*), granulocyte-macrophage colony-stimulating factor (*Csfgm*), and myosin heavy chain (*Myhs*) (Buchberg *et al.*, 1989; Ceci *et al.*, 1989; Okazaki *et al.*, 1993; McKenzie *et al.*, 1993). Recombination distances were calculated as described (Green, 1981) using the computer program SPRETUS MADNESS.

SSCP analysis. Primers (OCPIIMR1 and OCPIIML2) were designed to amplify a region corresponding to the 3′-untranslated region of the mouse *Ocp2* gene to test for single-strand conformation polymorphisms (SSCPs) between mouse strains. These were analyzed as previously described (Beier, 1993). Briefly, oligonucleotides (obtained from Research Genetics, Huntsville, AL) were radiolabeled with [^{32}P]ATP, and genomic DNAs from a series of mouse strains were amplified using standard protocols (94°C, 1 min, 55°C, 1 min, 72°C, 2 min for 40 cycles, with a final extension at 72°C). Two microliters of the amplified reaction is added to 8.5 μl stop solution (United States Biochemical Corp., Cleveland, OH), denatured at 94°C for 5 min, and immediately placed onto ice. Two microliters of each reaction is loaded on a 6% nondenaturing acrylamide sequencing gel and electrophoresed in 0.5× TBE buffer for 2–3 h at 40 W in a 4°C cold room. The pair OCPIIMR1 and OCPIIML2 identified a series of polymorphisms between the C57BL/6J and the *M. spretus* and therefore were used to analyze DNA prepared from the BSS backcross (Rowe *et al.*, 1994). The strain distribution pattern was analyzed using the Map Manager Program (Manly and Elliot, 1991).

RESULTS

Cloning of Ocp2, an Abundant cDNA in the Organ of Corti

Previous results showed that OCP-I and OCP-II are predominantly expressed in the mammalian inner ear and are among the most abundant proteins in the organ of Corti (Thalmann *et al.*, 1990). Cloning of these two genes should provide insight into their molecular function in the inner ear. Since the partial amino acid sequence of OCP-II was available (Thalmann *et al.*, 1993), we decided to clone the gene encoding OCP-II, which we named *Ocp2,* using the degenerate PCR method. Total RNA was isolated from guinea pig cochlea and reverse-transcribed into cDNA using random hexomers. The cDNA was used as the template for PCR using two degenerate oligos designed according to the partial peptide sequence. An apparent 250-bp PCR fragment was isolated from the agarose gel and cloned into pBluescript. Of the six independent colonies sequenced, one contained a 258-bp fragment, which, when translated, matched the internal OCP-II peptide sequence. The other five were unrelated sequences resulting from the degeneracy of the PCR condition. The cloned *Ocp2* fragment was radiolabeled to screen a cDNA library prepared from guinea pig organ of Corti (Wilcox and Fex, 1992). The primary screen identified OCP-II positives at a rate of about 1/1000. Although the library was previously amplified, this result was consistent with the original discovery that OCP-II is highly abundant in the organ of Corti (Thalmann *et al.*, 1980). Two different sizes of insert were identified,

900 and 1400 bp, respectively. The larger plasmid was named pSpoocp2A and the other pSpoocp2B.

Ocp-II Sequence Analysis

The two clones were sequenced in both directions. Both contained the complete coding region of *Ocp2* and were different in length only at the 3′-untranslated region, probably as a result of alternative splicing. The predicted open reading frame begins with a methionine codon at position 105 and ends with a TGA termination codon at nucleotide 594, encoding a protein of 163 amino acids with an estimated molecular mass of 18.6 kDa. The 3′-untranslated regions are 263 and 588 bp, respectively, with a potential polyadenylation signal (AATAAA) for the shorter transcript at position 823 and one (ATTAAA) for the larger transcript at position 1261 (Fig. 1A). Assignment of position 105 as the first nucleotide of the initiation codon agrees with the partial peptide sequence (Thalmann *et al.*, 1993). The amino acid composition of OCP-II is relatively acidic (23.3%). The abundance of acidic residues indicates that perhaps some are coordinating a metal or interacting with a basic surface. The other outstanding feature is the abundance of proline residues (amino acids 44–48 and 69–72). The prolines are suggestive of loop structures. The proline-rich domain of hepatocyte nuclear factor 1 has been shown to transactivate promoter-specific transcription of hepatitis B virus (Raney *et al.*, 1991). It has also been demonstrated that the SH3 binding sites of many proteins consist of a 10-amino-acid, proline-rich region (Ren *et al.*, 1993). Searching for motifs identified a putative ATP/GTP-binding site motif A (P-loop) starting at amino acid 129 (ANMIKGKT) (Hodgman, 1988a,b).

A search of the EMBL/GenBank databases revealed that OCP-II shares significant sequence similarity with the p15 subunit of a transcription factor named SIII. SIII was recently purified from mammalian cells and shown to regulate the activity of the RNA polymerase II elongation complex. SIII is a heterotrimer composed of 110-, 18-, and 15-kDa polypeptides and is capable of increasing the overall rate of RNA chain elongation by RNA polymerase II by suppressing transient pausing of the polymerase at multiple sites on the DNA template (Bradsher *et al.*, 1993a,b). The SIII p15 subunit encodes a 112-amino-acid, negatively charged polypeptide with a calculated molecular mass of 12.5 kDa (Garrett *et al.*, 1994). Alignments of OCP-II and p15 were shown in Fig. 1B. In a 61-amino-acid region of the amino-terminal half, these two proteins are 37% identical, 60% similar. In the other homologous region of 10 amino acids at the carboxyl-terminal half, these two peptides share 70% identity and 100% similarity. Besides the sequence homology, both proteins are negatively charged and their sizes are similar.

Tissue Expression of the OCP-II mRNA

To study the tissue distribution of the *Ocp2* mRNA with the extremely limited amount of RNA one could obtain from each cochlea, we adapted the RT-PCR method. Total RNA isolated from various tissues including brain, cochlea, eye, heart, intestine, kidney, liver, lung, thigh muscle, and testis were reverse-tran-

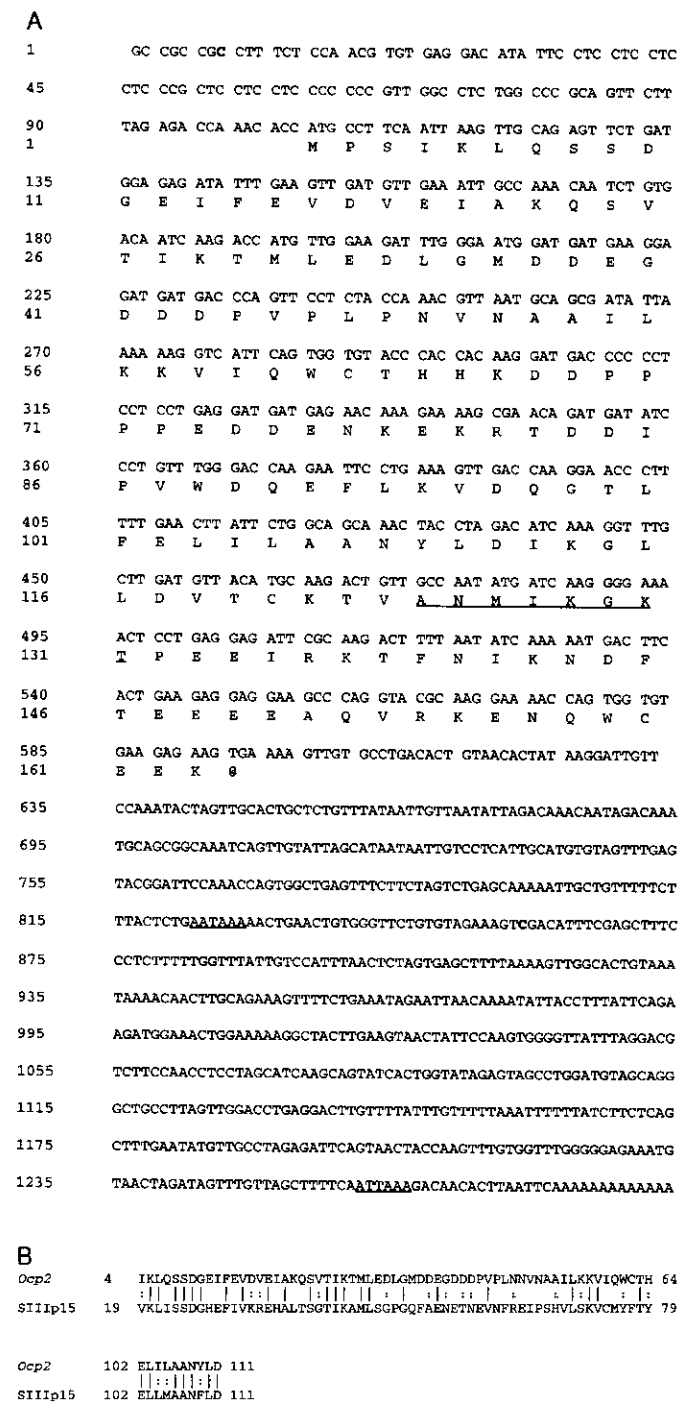

FIG. 1. (**A**) Nucleotide sequence and predicted amino acid sequence of the *Ocp2* cDNA clones. Nucleotides and amino acids are numbered on the left, and one-letter amino acid designations are used. The poly(A) signal sequences for both transcripts are underlined. The first and last nucleotides of the short transcript are indicated in boldface. The putative ATP/GTP-binding site motif A (P-loop) is underlined. (**B**) Alignments of *Ocp2* with SIIIp15. Sequences were aligned using the GAP program of the Genetics Computer Group package.

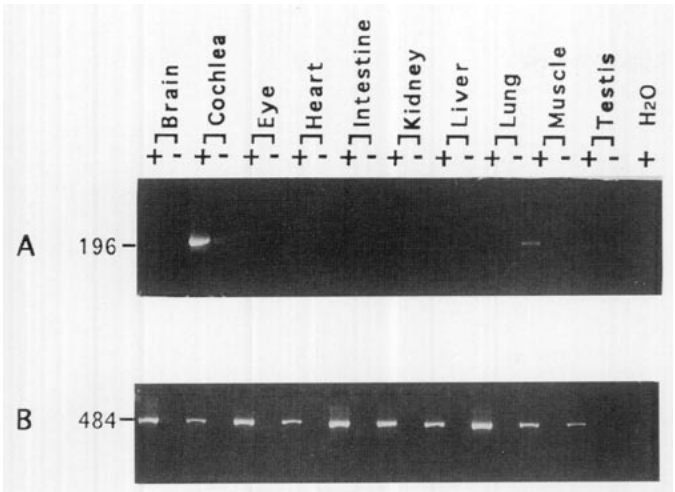

FIG. 2. RT-PCR analysis of *Ocp2* expression in different tissues. Total RNA was prepared from various tissues of guinea pig, reverse-transcribed, and amplified by PCR. (**A**) *Ocp2* primers; (**B**) P450 reductase primers as a positive control. +, with reverse transcriptase; −, same sample minus reverse transcriptase.

scribed, and PCR was performed under stringent conditions with a pair of primers covering most of the *Ocp2* coding region. As shown in Fig. 2A, *Ocp2* was predominately expressed in the cochlea, while only traces were detected in other tissues. A relatively more significant band was apparent in muscle, although it was not consistently as intensive in repeated experiments. In Fig. 2B, PCR reactions with a set of primers designed to amplify the guinea pig cytochrome P-450 reductase cDNA (Ohgiya *et al.*, 1992) were used with the same templates under identical PCR conditions, as a positive control to show that a comparable amount of cDNA was applied in each reaction and that PCR amplification worked in each sample prepared. The cytochrome P-450 reductase gene has been shown to be universally expressed in various tissues in guinea pig (Benedetto *et al.*, 1981; Katagiri *et al.*, 1989). The conclusion was that *Ocp2* is most abundantly expressed in the cochlea, but low expression in other tissues can also be observed with the high sensitivity of RT-PCR. Further studies are necessary to confirm the significance of the low expression and to understand the possible function implications.

Generation of an Antibody against OCP-II

A polyclonal antibody was raised against a synthetic tetradecapeptide corresponding to residues 3–16 of the amino acid sequence of OCP-II, coupled to keyhole limpet hemocyanin. This antibody was characterized by immunoprecipitation and immunoblot. The larger *Ocp2* plasmid pSpoocp2A was subjected to *in vitro* transcription and translation. The translational product was then immunoprecipitated with the polyclonal antibody. The major protein species detected had a relative molecular mass of ~22.5 kDa, which was consistent with that reported previously (Thalmann *et al.*, 1990). Immunoblot using freeze-dried samples of organ of Corti also detected a single band with the same molecular mass (Fig. 3). To understand further the function of the OCP-II protein, this polyclonal antibody was used in immunostaining.

Localization of OCP-II Protein by Immunostaining

Within the cochlea immunoreactive cells were conspicuous in the organ of Corti (Fig. 4D). Hair cells were only faintly stained but all adjacent nonsensory cells extending from interdental cells of the spiral limbus to root cells within the spiral ligament were darkly stained. A different pattern of staining was present within the vestibular portions of the inner ear. Supporting cells throughout the vestibular sensory epithelia were immunostained, but transitional cells in the adjacent epithelium showed a darker reaction (Figs. 4B and 4C). There was also reaction product on the remnants of the gelatinous membranes that overlie the sensory organs. A similar presence of reaction product on the interior surface of the tectorial membrane was sometimes found in the cochlea. There appeared to be less antigen present within the vestibular epithelia, based on the finding that between 5 and 10 times greater concentration of primary antibody was required to obtain staining in vestibular structures as dark as that found within the cochlea. The higher concentrations of primary antibody used to best demonstrate the vestibular structures were necessary to produce staining in neural structures. Peripheral neurons of Scapa's ganglion were stained (not shown). Observations within the brain were limited to the portion of the brain stem situated between the temporal bones. Within that area only neurons within the cochlear and vestibular nuclei were immunoreactive (Figs. 4E–4G). Within the ventral cochlear nucleus it appeared that all principal neurons were immunoreactive, with considerable variability in the degree of staining present (Fig. 4E). In contrast, within the dorsal cochlear nu-

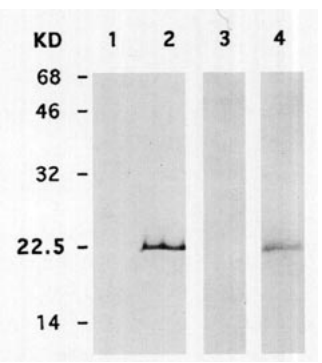

FIG. 3. Immunoprecipitation and immunoblots of OCP-II using anti-OCP-II serum. Lanes **1** and **2** show fluorographs of immunoprecipitates of *in vitro*-translated OCP-II protein with preimmune and anti-OCP-II serum raised against a synthetic peptide consisting of residues 3–16 of the amino acid sequence of OCP-II. Lanes **3** and **4** show immunoblots of guinea pig organ of Corti extracts with preimmune and anti-OCP-II serum.

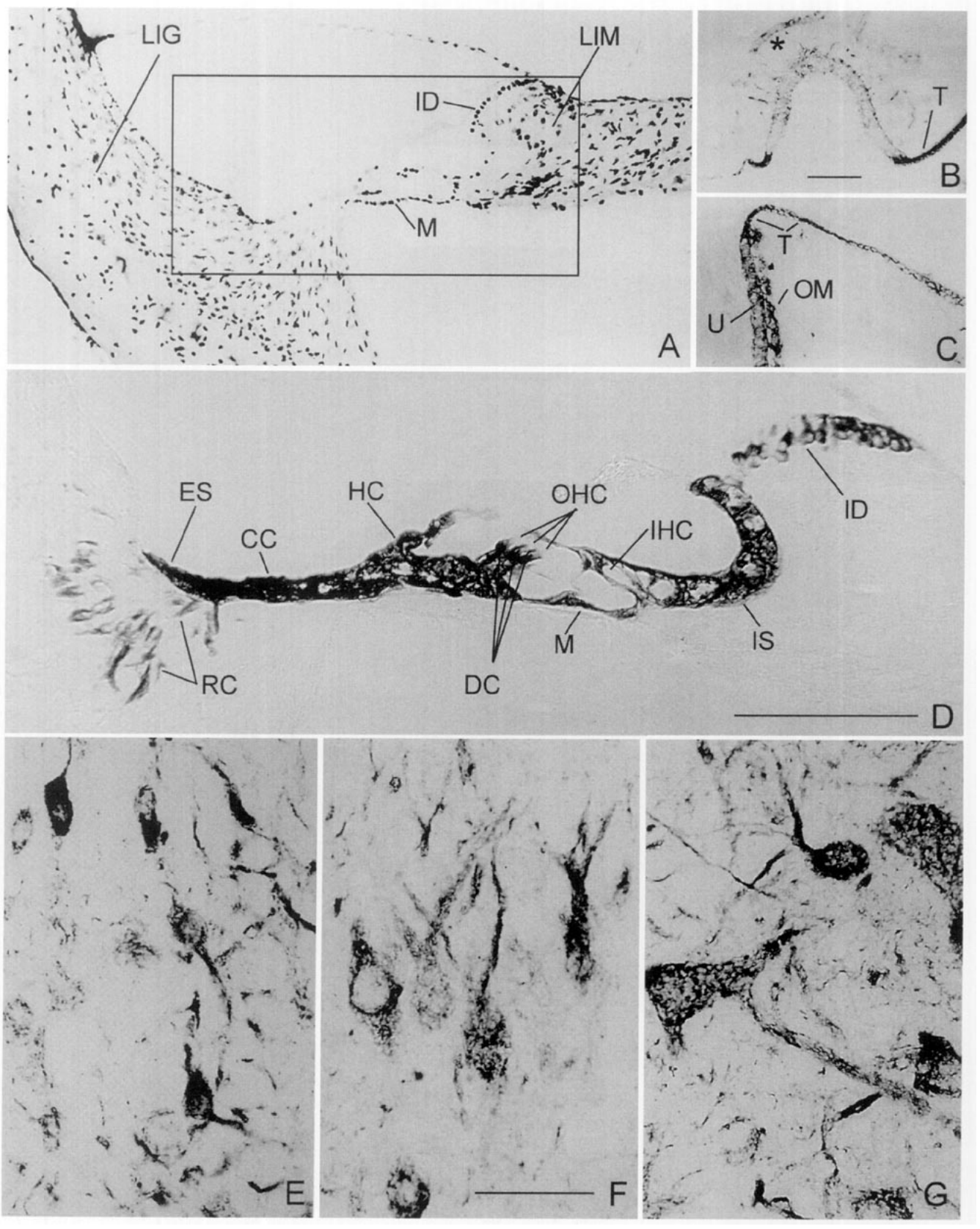

FIG. 4. Immunostaining of inner ear. (**A**) Cross section through the basal turn of a guinea pig cochlea stained for cell nuclei using Azure A. The enclosed area indicates the region shown at higher magnification in **D**. LIG, spiral ligament; LIM, spiral limbus; ID, interdental cells; M, mesenchymal cells lining the interior surface of the basilar membrane. (**B**) Cross section through a crista ampularis immunostained for OCP-II. The darkly stained cells on both sides of the base are transitional cells (T). The sensory epithelium lines the superior surface of the omega-shaped profile. The asterisk indicates reaction product on remnants of the cupula, which was destroyed by dehydration of the

cleus, of the variety of cell types present, only pyramidal cells (Fig. 4E) and large cells of the deep layers of the nucleus (not illustrated) were immunostained. All principal cells in the vestibular nuclei appeared to be immunoreactive (Fig. 4G). No immunostaining was present in any structure when either the preabsorbed antiserum or the preimmune antiserum were substituted for the primary antibody. The same staining pattern seen in the guinea pig organ of Corti was seen when cochleae of rat, gerbil, chinchilla, cat, pig, and human were immunostained (not illustrated).

Mapping of Ocp2

The restricted expression pattern of *Ocp2* in the auditory and vestibular organs as demonstrated above indicates that *Ocp2* may play an important role in inner ear function and is possibly a candidate gene for inherited hearing disorders. Mapping of *Ocp2* would provide a way to search for a disease caused by a defective *Ocp2* gene. To map in the mouse genomes, the mouse *Ocp2* homolog was cloned by RT-PCR using degenerate primers designed from the guinea pig sequence. Mouse and guinea pig *Ocp2* are 93% identical at the nucleotide level within the coding region and diverge completely in the 3′-untranslated region. However, the predicted amino acid sequence for mouse OCP-II is essentially identical to that of the guinea pig (data not shown). This result demonstrated that OCP-II is well conserved in evolution between the two species.

The murine chromosomal location of *Ocp2* loci was determined first by interspecific backcross analysis using progeny derived from matings of [C57BL/6J × *M. spretus*)F_1 × C57BL/6J] mice. This interspecific backcross mapping panel has been typed for over 1700 loci that are well distributed among all of the autosomes and the X chromosome (Copeland and Jenkins, 1991). C57BL/6J and *M. spretus* DNAs were digested with several restriction enzymes and analyzed by Southern blot hybridization for informative RFLPs using a probe derived from the 5′ end of the mouse *Ocp2* gene. The probe detected two independently segregating loci, *Ocp2*-related sequence locus-1 (*Ocp2-rs1*) and locus-2 (*Ocp2-rs2*). The mapping results indicated that *Ocp2-rs1* is located in the distal region of mouse chromosome 4 linked to *Fgr, Lag,* and *Nppa. Ocp2-rs2* is located in the central region of mouse chromosome 11 linked to *Adra1, Csfgm,* and *Myhs* (Fig. 5).

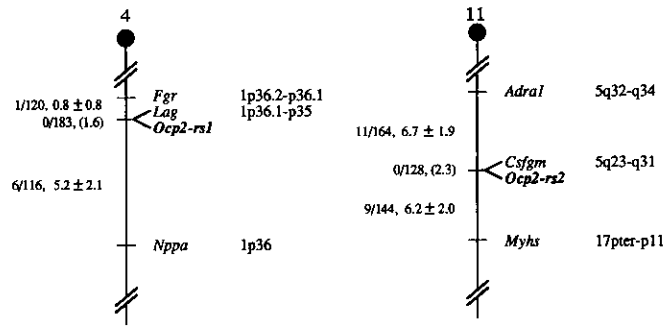

FIG. 5. Positions of the *Ocp2-rs1* and *Ocp2-rs2* loci on mouse chromosomes 4 and 11, respectively, determined by interspecific backcross analysis. Partial chromosome 4 and 11 linkage maps showing the locations of *Ocp2-rs1* and *Ocp2-rs2,* respectively, in relation to linked genes are illustrated. Gene order was determined by minimizing the number of recombination events required to explain the allele distribution patterns. No double recombinants were detected for any of the loci depicted on the maps; therefore, for the sake of brevity, haplotype data have not been included. The number of recombinant N_2 animals over the total number of N_2 animals typed plus the recombination frequencies, expressed as genetic distance in centimorgans (±1 SE), is shown for each pair of loci on the left of the chromosome maps. Where no recombinants were found between loci, the upper 95% confidence limit of the recombination distance is given in parentheses. The positions of loci in human chromosomes, where known, are shown to the right of the chromosome maps. References for the human map positions of loci cited in this study can be obtained from GDB (Genome Data Base), a computerized database of human linkage information maintained by The William H. Welch Medical Library of the Johns Hopkins University (Baltimore, MD).

SSCP analysis (Beier, 1993) was also applied to map *Ocp2* using primers corresponding to the 3′-untranslated region of the mouse *Ocp2* gene. An SSCP was identified between the C57BL/6J and the *M. spretus.* The BSS interspecific backcross was genotyped and the strain distribution pattern analyzed using the Map Manager program (Manly and Elliot, 1991). *Ocp2* was found to map to the distal region of chromosome 4 between D4Mit11 and D4Mit13, where *Fgr* and *Lag* are located (Abbott *et al.,* 1993). Because the more diverse 3′-untranslated region was used for this analysis, we concluded that the mouse *Ocp2* gene that we have cloned maps to chromosome 4, while a related sequence maps to chromosome 11.

The distal region of mouse chromosome 4 shares a region of homology with human chromosome 1 (summarized in Fig. 5). In particular, the human homolog for *Lag, LAP18,* has been assigned to 1p36.1–p35. The tight linkage between *Lag* and *Ocp2-rs1* in mouse sug-

organ. Calibration bar = 100 μm and applies to **B** and **C.** (**C**) Cross section of the macula of the utricle (U) with lightly stained supporting cells among the sensory cells. The adjacent transitional cells (T) are more darkly stained than the sensory epithelium. There is reaction product on remnants of the otolithic membrane (OM), which was destroyed by the dehydration process. (**D**) Immunostained organ of Corti and adjacent nonsensory cells. ID, interdental cells of the spiral limbus; IS, inner sulcus cells; IHC, inner hair cell; OHC, outer hair cells; M, mesenchymal cells as in **A;** DC, Deiter's cells; HC, Hensen's cells; CC, Claudlus cells; ES, external sulcus cells; RC, root cells. Calibration bar = 100 μm. (**E**) Horizontal section through the middle of the ventral cochlear nucleus showing heterogeneity in the size of positively stained cells and variability in the degree of their staining. (**F**) Horizontal section through the dorsal cochlear nucleus showing positively stained cytoplasm and dendrites of pyramidal cells. Calibration bar = 100 μm. (**G**) Horizontal section through the lateral vestibular nucleus showing positive staining of the principal cells.

gests that the human homolog of *Ocp2-rs1* will reside on 1p36. The central region of mouse chromosome 11 shares a region of homology with human chromosomes 5 and 17 (summarized in Fig. 5). The human homolog for *Csfgm, CSF2,* lies on 5q23–q31. Therefore, we predict that the human homolog of *Ocp-rs2* will map to the long arm of human chromosome 5.

DISCUSSION

Functions of different organs are expressed through the expression of specific proteins. Proteins intimately associated with specific functions of particular cells have been identified in numerous systems. For example, hemoglobin, the oxygen carrier protein, is exclusively and abundantly present only in red blood cells. As part of our effort to understand the molecular basis of cochlear function, we have cloned a novel gene, *Ocp2,* from a guinea pig organ of Corti cDNA library. The *Ocp2* messenger RNA is expressed most abundantly in the cochlea while not significantly in any other tissues as examined by RT-PCR, including brain, eye, heart, intestine, kidney, liver, lung, thigh muscle, and testis. Immunohistochemical staining of paraffin-embedded sections with a polyclonal antiserum raised against the N-terminal peptide of OCP-II demonstrates that OCP-II is abundant in nonsensory cells in the organ of Corti. It is also localized, at lower concentrations, in vestibular end organs and in selected ganglion cells of the auditory and vestibular nuclei. It should be remembered, though, that within the brain, this study was restricted to the portion of the brain stem between the temporal bones. OCP-II was observed by immunostaining in all of the mammalian species examined.

Analysis of its deduced amino acid sequence revealed that the OCP-II protein shares significant sequence similarity with p15, a subunit of transcription factor SIII. It was demonstrated that SIII functions through a direct interaction with the RNA polymerase II elongation complex to stimulate the overall rate of RNA chain elongation by suppressing transient pausing of the polymerase at multiple sites on the DNA template (Bradsher *et al.,* 1993a,b). The particular role of the p15 subunit is speculative, possibly involved in RNA binding (Garrett *et al.,* 1994).

Our discovery that *Ocp2* is predominantly and highly expressed in auditory organs indicates that it may serve an important function in the inner ear. The demonstration that OCP-II is evolutionarily conserved among different mammalian species also supports this hypothesis. In general, OCP proteins, including OCP-I and OCP-II, may serve as structural proteins. The finding of immunoreactivity in the endolymphatic spaces suggests that OCP-II may be secreted apically by immunoreactive cells. As demonstrated above, although present at very different concentrations, OCP-II can be identified in many different cell types located in auditory and vestibular end organs, as well as many neurons. Therefore, while OCP-II expression is limited to the components of the central and peripheral auditory and vestibular organs, one cannot make a definitive correlation as to its role. The exclusive localization of OCP-II immunostaining within cochlear nonsensory epithelial cells was striking because these same cells have recently been shown to form a system coupled by gap junctions (Kikuchi *et al.,* 1995). The morphological arrangement of the cells, together with the presence of ion transport enzymes at key sites, suggests that this system of cells plays an essential role in recycling potassium ions from the basolateral surfaces of hair cells back to the endolymphatic space. The presence of OCP-II immunostaining throughout this system suggests a possible role of OCP-II in the specialized function of these cells. Similarly, in vestibular organs OCP-II immunostaining was found within nonsensory cells that are connected via gap junctions. Differences in the arrangement of auditory and vestibular gap junction systems (Kikuchi *et al.,* 1994), and correspondingly in the arrangement of OCP-II positive cells, probably reflect the pronounced difference between the organs in the presence of the high endolymphatic potential that is unique to the cochlear endolymphatic space (Smith *et al.,* 1958) and the attendant specializations that are necessary for recycling ions into this space.

An alternative hypothesis is that OCP-II plays an important role in transcription regulation for the development or maintenance of the specialized functions of the inner ear. The finding that it shares homology with a transcription subunit provides us the first evidence of OCP-II being a putative transcription-associated factor. Besides its homology to SIIIp15, several additional features of OCP-II, such as its acidic nature and proline-rich domains, also suggest a possible role for OCP-II in transcription regulation. Studies of *Ocp2* expression and regulation during mouse embryo development could provide evidence for the hypothesis. Further biochemical experiments will also be required to establish that OCP-II functions as part of the transcriptional apparatus. Experiments using transgenic techniques will be necessary to elucidate eventually the biological function of *Ocp2.*

Identification of genes like *Ocp2* provides potential candidates for genetically determined syndromes of hearing loss in human and mouse. The *Ocp2* loci were mapped to mouse chromosome 4 and chromosome 11. When comparing our interspecific map of chromosomes 4 and 11 with the composite mouse linkage map that reports the map location of many uncloned mouse mutations [compiled by M. T. Davisson, T. H. Roderick, A. L. Hillyard, and D. P. Doolittle and provided from GBASE (a computerized database maintained at The Jackson Laboratory, Bar Harbor, ME)], we found only one mouse mutant, *jerker* (*je*), that affects the inner ear. However, our data exclude *Ocp2-rs1* as the candidate gene for *je,* since a high-resolution map of the *je* region indicated that *Ocp2-rs1* lies several centimorgans proximal to the *je* locus (H. Chen, unpublished observations). *Shaker-2* (*sh-2*) is the only inner ear mu-

tation that maps to the central region of chromosome 11. The relationship between *Ocp2-rs2* and *sh-2* is being investigated.

Finally, the *Ocp2* gene will be useful in studies of the inner ear development, because its expression is specifically related to the inner ear. The product of *Ocp2* can serve as an *in situ* cellular marker for the inner ear. The relatively restricted pattern of *Ocp2* gene transcription suggests that analysis of its promoter will provide additional insights as well as tools for studies of the auditory organs. For example, the promoter can be useful for gene transfer and gene therapy experiments.

ACKNOWLEDGMENTS

We are deeply grateful to Tom Brody for providing automated DNA sequencing. We are also thankful to Dr. J. Jiang for her advice on the protein work and Dr. T. Ellenberger for his advice on sequence and protein structure analysis. We thank D. J. Gilbert, D. Swing, M. Barnstead, and D. Barnhart for excellent assistance. This research was supported by the Howard Hughes Medical Institute; in part, by the National Cancer Institute, DHHS, under Contract NO1-CO-74101 with ABL; by NIH, National Research Service Award 5F32GM15909-02 from the National Institute of General Medical Sciences (K.B.A.); by NIDCD/NIH Grants R01 00269 in part (J.C.A.), DC01374 (I.T.), and DC01414 (R.T.); and by RO1 HD29028 from NICHD and RO1 HG00951 from the NCHGR (D.R.B.).

REFERENCES

Abbott, C. M., Blank, R., Eppig, J. T., Fiedorek, F. T., Jr., Frankel, W., Friedman, J. M., Huppi, K. E., Jackson, I., Steel, K., Mock, B. A., Stoye, J., and Seman, R. W. (1993). Mouse chromosome 4. *Mamm. Genome* **4:** S58–S71.

Adams, J. C. (1992). Biotin amplification of biotin and horseradish peroxidase signals in histochemical stains. *J. Histochem. Cytochem.* **40:** 1457–1463.

Beier, D. R. (1993). Single-strand conformation polymorphism (SSCP) analysis as a tool for genetic mapping. *Mamm. Genome* **4:** 627–631.

Beier, D. R., Dushkin, H., and Sussman, D. J. (1992). Mapping genes in the mouse using single-strand conformation polymorphism analysis of recombinant inbred strains and interspecific crosses. *Proc. Natl. Acad. Sci. USA* **89:** 9102–9106.

Benedetto, C., Dianzani, M. U., Ahmed, M., Cheeseman, K., Connelly, C., and Slater, T. F. (1981). Activation of carbon tetrachloride, and distribution of NADPH-cytochrome C reductase, cytochrome P-450, and other microsomal enzyme activities in rat tissues. *Biochim. Biophys. Acta* **677:** 363–372.

Bradsher, J. N., Jackson, K. W., Conaway, R. C., and Conaway, J. W. (1993a). RNA polymerase II transcription factors SIII. I. Identification, purification, and properties. *J. Biol. Chem.* **268:** 25587–25593.

Bradsher, J. N., Tan, S., McLaury, H.-J., Conaway, J. W., and Conaway, R. C. (1993b). RNA polymerase II transcription factor SIII. II. Functional properties and role in RNA chain elongation. *J. Biol. Chem.* **268:** 25594–25603.

Buchberg, A. M., Brownell, E., Nagata, S., Jenkins, N. A., and Copeland, N. G. (1989). A comprehensive genetic map of murine chromosome 11 reveals extensive linkage conservation between mouse and human. *Genetics* **122:** 153–161.

Ceci, J. D., Siracusa, L. D., Jenkins, N. A., and Copeland, N. G. (1989). A molecular genetic linkage map of mouse chromosome 4 including the localization of several proto-oncogenes. *Genomics* **5:** 699–709.

Chomczynski, P., and Sacchi, N. (1993). Guanidinium methods for total RNA preparation. *In* "Current Protocols in Molecular Biology" (F. M. Ausubel, R. Brent, R. E. Kingston, D. D. Moore, J. G. Seidman, J. A. Smith, and K. Struhl, Eds.), pp. 4.2.4–4.2.8, Wiley, New York.

Compton, T. (1990). Degenerate primers for DNA amplification. *In* "PCR Protocols" (M. A. Innis, D. H. Gelfand, J. J. Sninsky, and T. J. White, Eds.), pp. 39–45, Academic Press, San Diego, CA.

Copeland, N. G., and Jenkins, N. A. (1991). Development and applications of a molecular genetic linkage map of the mouse genome. *Trends Genet.* **7:** 113–118.

Corey, D. P., and Hudspeth, A. J. (1979). Ionic basis of the receptor potential in a vertebrate hair cell. *Nature* **281:** 675–677.

Garrett, K. P., Tan, S., Bradsher, J. N., Lane, W. S., Conaway, J. W., and Conaway, R. C. (1994). Molecular cloning of an essential subunit of RNA polymerase II elongation factor SIII. *Proc. Natl. Acad. Sci. USA* **91:** 5237–5241.

Green, M. C. (1981). Linkage, recombination and mapping. *In* "Genetics and Probability in Animal Breeding Experiments," pp. 77–113, Oxford Univ. Press, New York.

Hodgman, T. C. (1988a). A new superfamily of replicative proteins. *Nature* **333:** 22–23.

Hodgman, T. C. (1988b). A new superfamily of replicative proteins (Erratum). *Nature* **333:** 578.

Jenkins, N. A., Copeland, N. G., Taylor, B. A., and Lee, B. K. (1982). Organization, distribution, and stability of endogenous ecotropic murine leukemia virus DNA sequences in chromosomes of *Mus musculus*. *J. Virol.* **43:** 26–36.

Jiang, J. X., White, T. W., Goodenough, D. A., and Paul, D. L. (1994). Molecular cloning and functional characterization of chick lens fiber connexin 45.6. *Mol. Biol. Cell* **5:** 363–373.

Katagiri, M., Sugiyama, T., Tsutsukawa, N., Ishiguro, H., Miyoshi, N., Ishibashi, F., and Taniguchi, N. (1989). Comparative studies on microsomal NADPH-cytochrome P-450 reductase using a monoclonal antibody: Tissue distribution, specific activity and peptide mapping. *Int. J. Biochem.* **21:** 1395–1405.

Kikuchi, T., Adams, J. C., Paul, D. L., and Kimura, R. K. (1994). Gap junction systems in the rat vestibular labyrinth: Immunohistochemical and ultrastructural analysis. *Acta Otolaryngol. (Stockh.)* **114:** 520–528.

Kikuchi, T., Kimura, R. K., Paul, D. P., and Adams, J. C. (1995). Gap junctions in the rat cochlea: Immunohistochemical and ultrastructural analysis. *Anat. Embryol.* **191:** 101–118.

Manly, K. F., and Elliott, R. W. (1991). RI Manager, a microcomputer program for the analysis of data from recombinant inbred strains. *Mamm. Genome* **1:** 123–126.

Marcus, D. C. (1986). Non-sensory electrophysiology of the cochlea: Stria vascularis. *In* "Neurobiology of Hearing: The Cochlea" (R. A. Altschuler, D. W. Hoffman, and R. P. Bobbin, Eds.), pp. 123–137, Raven Press, New York.

McKenzie, A. N., Li, X., Largaespada, D. A., Sato, A., Kaneda, A., Zurawski, S. M., Doyle, E. L., Milatovich, A., Francke, U., Copeland, N. G., Jenkins, N. A., and Zurawski, G. (1993). Structural comparison and chromosomal localization of the human and mouse IL-13 genes. *J. Immunol.* **150:** 5436–5444.

Ohgiya, S., Goda, T., Ishizaki, K., Kamataki, T., and Shinriki, N. (1992). Molecular cloning and sequence analysis of mouse NADPH-cytochrome p450 oxidoreductase. *Biochim. Biophys. Acta* **1171:** 103–105.

Okazaki, T., Yoshida, B. N., Avraham, K. B., Wang, H., Wuenschell, C. W., Jenkins, N. A., Copeland, N. G., Anderson, D. J., and Mori, N. (1993). Molecular diversity of the SCG10/stathmin gene family in the mouse. *Genomics* **18:** 360–373.

Orita, M., Suzuki, Y., Sekiya, T., and Hayashi, K. (1989). Rapid and

sensitive detection of point mutations and DNA polymorphisms using the polymerase chain reaction. *Genomics* **5:** 874–879.

Raney, A. K., Easton, A. J., Milich, D. R., and McLachlan, A. (1991). Promoter-specific transactivation of Hepatitis B virus transcription by a glutamin- and proline-rich domain of Hepatocyte nuclear factor 1. *J. Virol.* **65:** 5774–5781.

Ren, R. Mayer, B. J., Cicchetti, P., and Baltimore, D. (1993). Identification of a ten-amino acid proline-rich SH3 binding site. *Science* **259:** 1157–1161.

Rowe, L. B., Nadeau, J. H., Turner, R., Frankel, W. N., Letts, V. A., Eppig, J. T., Ko, M. S., Thurston, S. J., and Birkenmeier, E. H. (1994). Maps from two interspecific backcross DNA panels available as a community genetic mapping resource. *Mamm. Genome* **5:** 253–274.

Salt, A. N., and Konishi, T. (1986). The cochlear fluids: Perilymph and endolymph. *In* "Neurobiology of Hearing: The Cochlea" (R. A. Altschuler, D. W. Hoffman, and R. P. Bobbin, Eds.), pp. 109–122, Raven Press, New York.

Smith, C. A., Davis, H., Deatherage, B. H., and Gessert, C. F. (1958). DC potentials of the membranous labyrinth. *Am. J. Physiol.* **193:** 203–206.

Sterkers, O. (1985). Origin and electrochemical composition of endolymph in the cochlea. *In* "Auditory Biochemistry" (D. G. Drescher, Ed.), pp. 473–487, Thomas, Springfield, IL.

Thalmann, I., Rosenthal, H. L., Moore, B. W., and Thalmann, R. (1980). Organ of Corti-specific polypeptides: OCP-I and OCP-II. *Arch. Oto-Rhino-Laryngol.* **226:** 123–128.

Thalmann, I., Suzuki, H., McCourt, D. W., Comegys, T. H., and Thalmann, R. (1993). Partial amino acid sequences of organ of Corti proteins OCP1 and OCP2: A progress report. *Hearing Res.* **64:** 191–198.

Thalmann, I., Takahashi, K., Varghese, J., Comegys, T. H., and Thalmann, R. (1990). Biochemical features of major organ of Corti proteins (OCP-I and OCP-II) including partial amino acid sequence. *Laryngoscope* **100:** 99–105.

Thalmann, R. (1976). Quantitative histo- and cytochemistry of the ear. *In* "The Handbook of Auditory and Vestibular Research Methods," Part III, "Biochemistry" (C. A. Smith and J. A. Vernon, Eds.), pp. 359–419, Thomas, Springfield, IL.

Towbin, H. T., Staehelin, T., and Gordon, J. (1979). Electrophoretic transfer of protein from polyacrylamide gels to nitrocellulose sheets: Procedure and some applications. *Proc. Natl. Acad. Sci. USA* **76:** 4350–4354.

Wilcox, E. R., and Fex, J. (1992). Construction of a cDNA library from microdissected guinea pig organ of Corti. *Hearing Res.* **62:** 124–126.